Received April 22, 2021, accepted May 18, 2021, date of publication May 25, 2021, date of current version June 4, 2021.

Digital Object Identifier 10.1109/ACCESS.2021.3083698

A Stochastic Planning Model for Improving Resilience of Distribution System Considering Master-Slave Distributed Generators and Network Reconfiguration

MOSTAFA GHASEMI[1], AHAD KAZEMI[1], MOHAMMAD AMIN GILANI[1], AND MIADREZA SHAFIE-KHAH[2], (Senior Member, IEEE)

[1]Centre of Excellence for Power System Automation and Operation, Department of Electrical Engineering, Iran University of Science and Technology, Tehran 16846-13114, Iran

[2]School of Technology and Innovations, University of Vaasa, 65200 Vaasa, Finland

Corresponding authors: Ahad Kazemi (kazemi@iust.ac.ir) and Miadreza Shafie-Khah (mshafiek@uwasa.fi)

ABSTRACT The recent experiences of extreme weather events highlight the significance of boosting the resilience of distribution systems. In this situation, the resilience of distribution systems planning leads to an efficient solution for protecting the system from these events via line hardening and the installation of distributed generators (DGs). For this aim, this study presents a new two-stage stochastic mixed-integer linear programming model (SMILP) to hedge against natural disaster uncertainty. The first stage involves making investment decisions about line hardening and DG installation. Then, in the second stage, the dynamic microgrids are created according to a master-slave concept with the ability of integrating distributed generators to minimize the cost of loss of load in each uncertain outage scenario. In particular, this paper presents an approach to select the line damage scenarios for the SMILP. In addition, the operational strategies such as load control capability, microgrid formation and network reconfiguration are integrated into the distribution system plans for resilience improvement in both planning and emergency response steps. The simulation results for an IEEE 33-bus test system demonstrate the effectiveness of the proposed model in improving disaster-induced the resilience of distribution systems.

INDEX TERMS Distribution system, two-stage stochastic programming, resilience improvement planning, master-slave concept, microgrid formation.

NOMENCLATURE

Indices

d	Block index
e	Energy storage index
b, b'	Bus indices
k	Microgrid index
l, l'	Distribution line indices
m	DG index
ω	Scenario index
t	Time index

Sets

Ω_L	Set of lines l
$\Omega_{L'}$	Set of lines l' without switch
$\Omega_{B_{\mathrm{MDG}}}$	Set of buses connected to the master DGs
Ω_{E}	Set of energy storage units
Ω_{IB}	Set of initial buses of line l
$\Omega_{\mathrm{N}}, \Omega_{\mathrm{NC}}$	Set of candidate and non-candidate buses
Ω_{TB}	Set of terminal buses of line l
Ω_{K}	Set of formable microgrids
Ω_{B}	Set of loads
Ω_{M}	Set of DGs
Ω_{I}	Set of lines connected to bus b
Ω_{ω}	Set of scenarios

Parameters

B	Limited budget
BM	A sufficiently big number
c^{dg}	Capital cost ($) for installing a DG

The associate editor coordinating the review of this manuscript and approving it for publication was Anamika Dubey.

c_l^h	Capital cost ($) of hardening line l
$c_{b,t}^{ls}$	Penalty cost ($) for load shedding
Cap_e^{ES}	Energy storage capacity
$DR_{j,t}^{L,Max}$	Maximum load control limit
$E1_l, E2_l$	Electrical characteristic of line
$HB_{b,s}$	Binary parameter indicating bus health
$HE_{l,\omega}$	Binary parameter indicating line health
$MapTL_{i,l}$	Parameter indicating the power of injection to a line
p_{cond}	Conductor failure probability
$P_{b,t}$	Predicted active load (kW)
$P_{j,d,t,\omega}^b$	Load control blocks
p_l	Failure probability of line l
P_l^{Max}	Active power flow (kW) limits of a line
$P_m^{DG,Max}$	Maximum active power (kW) limit of a DG
p_{pole}	Failure probability of a pole
$Q_{b,t}$	Predicted reactive load (kvar)
Q_l^{Max}	Reactive power flow (kvar) limits of a line
$Q_m^{DG,Min}, Q_m^{DG,Max}$	Minimum and maximum reactive power (kvar) limits of a DG
r_l, x_l	Resistance and reactance (pu) of line l
$Rate_e^{ch,\max}$	Maximum charge rate of energy storage
$Rate_e^{dch,\max}$	Maximum discharge rate of energy storage
$SOC_e^{ES,initial}$	Initial state of charge of energy storage
$SOC_e^{ES,\max}$	Maximum SOC of energy storage
$SOC_e^{ES,\min}$	Minimum SOC of energy storage
$V_k^{DG,set}$	Voltage magnitude of buses connected to master DGs
V^{min}, V^{max}	Minimum and maximum voltage of a bus
$z_{l,s}$	Binary parameter indicating that line l is damaged in scenario ω
δ^{max}	Maximum limit of voltage angle
ε	A small amount
η_e^{ES}	Energy storage efficiency
ρ_ω	Probability of each scenario
φ_h	Average occurrences of hurricanes in a year

Variables

$p_{b,k,t,\omega}^L$	Scheduled active loads
$p_{j,k,t,\omega}^{LC}$	Scheduled active load control
$p_{l,t,\omega}$	Active power flow (kW) of lines
$p_{m,k,t,\omega}^{DG}$	Scheduled active power of DGs
$p_{m,b,k,t,\omega}^{DG,dep}$	Linearized active power generation of DGs
$pes_{e,k,t,\omega}^{ch}$	Charging power of energy storage
$pes_{e,k,t,\omega}^{dch}$	Discharging power of energy storage
$q_{l,t,\omega}$	Reactive power flow (kvar) of lines
$q_{m,b,k,t,s}^{DG,dep}$	Linearized reactive power generation of DGs
$soc_{e,k,t,\omega}^{ES}$	SOC of energy storage
$v_{b,k,t,\omega}$	Bus voltage magnitude
$zp_{l,t,\omega}$	Active power equality constraint slack variables
$zq_{l,t,\omega}$	Reactive power equality constraint slack variables
$\delta_{b,k,t,\omega}$	Bus voltage angles
$\Delta P_{j,k,t,\omega}^{LC}$	Difference between scheduled and deployed load control
$\Delta P_{m,k,t,\omega}^{DG}$	Difference between scheduled and output power of DGs
$\gamma_{b,k,\omega,m}$	Linearization variable
$\gamma_{e,k,t,\omega}^{ES}$	Status of energy storage
$\sigma_{j,d,t,\omega}^{L}$	Scheduled block for the load controls

Binary variables

Y_l	1 if distribution line l is hardened; 0 otherwise
Z_m	1 if a back-up DG m is installed; 0 otherwise
$Z_{m,b}^{EM}$	1 if a back-up DG m is placed at bus b; 0 otherwise
$\alpha_{b,k,\omega}$	Binary variable indicating that bus b belongs to microgrid k
$\beta_{l,\omega}$	1 if line is active; 0 otherwise
$\beta_{l,k,\omega}$	1 if line in microgrid k is active; 0 otherwise
$\lambda_{k,\omega}$	Fictional flows on the distribution line l
$\xi_{b,b',l,k,\omega}^{(1)}$	Binary variable for microgrid formation
$\xi_{b',k,\omega}^{(2)}$	Fictional supply of master DG

Abbreviations

SOC	State of charge
ES	Energy storage
DR	Demand response
DG	Distributed generator
IGDT	Information gap decision theory
SMILP	Stochastic mixed-integer linear programming

I. INTRODUCTION

Extreme weather conditions in recent years have resulted in long and widespread electricity service interruptions with enormous economic losses [1]. For example, Hurricane Harvey resulted in power interruptions that affected several million customers in Texas for 14 days [2]. Unfortunately, it has been predicted that the frequency and intensity of extreme weather events such as floods and hurricanes are expected to rise as a result of climate change [3]. Therefore, in order

to improve the resilience of distribution systems, three types of strategies including planning, pre-natural disasters actions, and operational can be adopted [4]. Improving the resilience of electricity distribution systems against extreme weather events through planning measures has been a critical issue for power network operations. The additional investment in distribution network resilience can reduce additional operational costs due to extreme weather events. In this regard, hardening vulnerable distribution lines and installing distributed generators (DGs) are effective defensive measures taken by utilities for resilience improvement.

Hardening distribution lines with stronger materials can reduce their vulnerability to natural disasters, thereby enabling them to supply the critical loads [5], [6]. In addition, during extreme weather events, such as a hurricane, because of the probability of losing the main grid, the controllable generators can supply power for the critical loads and form self-supplied microgrids to increase load restoration capabilities after an extreme weather event [7], [8]. Therefore, the development of a resilient distribution system planning model for the optimal design of planning measures can considerably decrease the negative impacts of natural disasters.

Evidently, the resilient distribution system planning issue is related to a high level of uncertainty. Information gap decision theory (IGDT) and robust and stochastic optimization frameworks are already utilized as three types of uncertainty modeling to tackle this challenge. In [9], a strategy based on IGDT technique was introduced to facilitate decision making for distribution system planners upon the occurrence of natural disasters. In [10], a tri-level planner-disaster-risk-averse-planner model was introduced for planning in integrated natural gas and power networks exposed to extreme disasters. That work utilizes IGDT optimization technique to improve the resilience of the integrated system under extreme events. In [11], a multi-scenario two-stage distributively robust planning model was presented to hedge against random offensive resources of natural disasters and line outage uncertainties. In the first stage, the distribution system is protected from natural disasters through pre-planned distributed generation allocation and line hardening. Also, microgrid formation and network reconfiguration are employed to enhance the operational resilience of distribution systems in the second stage. In [12], a planning-attack-reconfiguration optimization model was proposed to enhance the resilience of distribution systems and fight against natural disasters. In [6], a tri-level optimal hardening model was presented to improve the resilience of distribution systems in the face of malicious attacks. However, the IGDT technique and robust optimization can be overly conservative and computationally cumbersome in resilient distribution system planning. Stochastic programming, as an effective means for uncertainty handling, generates representative scenarios for line damage modeling. In [13], a stochastic programming model was proposed to allocate limited budget to the hardening of distribution networks. In [14], a two-stage stochastic mixed integer model was proposed for protecting distribution networks in the face of extreme weather events. The first stage involved the identification of the resilience-oriented design decisions by the model. In the second stage, the mid- and post-event system operation cost and the damage repair cost were evaluated. In [15], a two-stage stochastic optimization model was proposed for designing resilient distribution systems by deploying various options such as the hardening of existing lines, installing DGs, building new lines, and adding switches. This work considered line damage scenarios depending on extreme weather as a stochastic event for assessment of the distribution system performance in the wake of a disaster. In [16], a stochastic mixed integer programming model was proposed to boost the resilience of distribution systems by installing fuel-based distributed generator. In [17], a novel planning model is proposed to capture the effects of investment measures and uncertainties over three stages on microgrid formation problem. According to this model, the investment measures are defined in the first stage. Then, the provisional microgrids are formed based on the line outage scenarios in the second stage and the load shedding cost in each microgrid is minimized based on the load scenarios in the third stage. However, this work did not consider the limited hardening budget in the planning model. In addition, the line damage scenarios are generated based on the worst-case event.

Moreover, the distribution systems resilience can be improved by post-event operational strategies of load control capability, network reconfiguration and microgrid formation. In [18], a probabilistic method was presented to minimize network's aging and maximize its reliability by using the emergency demand response program. In [19], a model was proposed to investigate the impact of demand response on the resilience of dynamic clustered distribution system in operation stage. In addition, network reconfiguration is an effective strategy to pick up critical loads after natural disasters. In [20], a multi-stage stochastic optimization model was proposed for jointly wind turbine allocation and network reconfiguration in a multi-fault system. In [21], a bi-level network reconfiguration model was presented to improve the electricity distribution network resilience against severe weather events such as hurricane.

A number of stochastic distribution system planning works have addressed the microgrid form, resulting in an improvement in the system resilience. However, none of these studies have considered the formation of microgrids based on the master-slave control technique with the capability of integrating DGs. Microgrid formation is one of the most effective operational strategies for improving the resilience of distribution systems. The lessons learned from extreme events show microgrids are an appropriate measure to improve resilience. During the 2011 earthquake and tsunami in Japan, the Sendai microgrid survived for two days without the upstream network [22]. In [23], a two-stage optimization model was proposed to optimize investment in mobile energy storage units in the first stage and form dynamic microgrids to avoid load

TABLE 1. Comparisons between the presented method and other existing planning methods.

References	Power Flow	Planning measures		Uncertainty modeling			Operational Strategies			
		Line hardening	DG placement	IGDT	Robust	Stochastic	Microgrid formation	Integration of master and slave units	reconfiguration	Demand response
[4]	AC-OPF	✓				✓	✓		✓	
[6]	DistFlow	✓			✓		✓		✓	
[9]	DistFlow	✓	✓	✓					✓	
[12]	AC-PF		✓		✓				✓	
[16]	AC-OPF		✓			✓				
[25]	DistFlow	✓	✓			✓	✓		✓	
[26]	AC-OPF	✓	✓			✓	✓		✓	
This paper	AC-OPF	✓	✓			✓	✓	✓	✓	✓

shedding in the second stage. In [24], a two-stage framework consisting of mobile emergency generator pre-positioning and real-time allocation was proposed to restore critical loads via the formation of multiple microgrids. References [23] and [24] did not adopt line hardening and distributed generation allocation as investment decisions in the resilient planningmodel. Ref. [4] presented a stochastic programming model in order to boost the resilience planning of integrated power distribution system and water distribution system against earthquakes. In [25], a novel two-stage stochastic optimization approach strategy was formulated to assess the effects of investment decisions and investment uncertainties on the performance of a distribution system both during and after the occurrence of emergency conditions. This work presented a hybrid stochastic process and deterministic causal structure to accommodate the correlations of various uncertainties. In [26], a two stage stochastic optimization model was introduced to enhance the resilience of the distribution system by using a social welfare index. This work obtained the operation state of the distribution equipment through a comparison of the failure probability of components with a uniform random number. These works did not consider the master-slave distributed generator concept and distributed energy resources in the resilient distribution system planning model. Comparisons between the presented method and other existing planning methods for the resilience of distribution systems improvement is presented in Table 1, which includes Power Flow (PF), resilience measures, uncertainty modeling and operational strategies.

To address the above shortcomings, this paper proposes a novel stochastic planning model with the operational strategies such as microgrid formation and load control capability to reduce the load interruptions when the main grid is available. To sum up, the key contributions of the proposed method are as follows:

- A novel linear two-stage stochastic process is presented for resilient distribution system planning considering line damage uncertainty; thus, this method can increase the strength of infrastructure and enable self-healing operation.
- The planning measures and the operational strategies such as microgrid formation, load control capability and network reconfiguration are integrated with line damage uncertainty over two stages to enhance the distribution systems resilience. To the best of our knowledge, the impact of the master-slave technique and load control capability on resilient distribution system planning has not been considered in previous works. Therefore, a comprehensive formulation based on a master-slave method with the ability of integrating DGs is presented to model the microgrid formation problem.
- In the second stage of the proposed model, the self-healing operation can reduce the outage propagation in the distribution network until sectionalizers disconnect the lines. This method sectionalizes the distribution network into multiple self-supplied microgrids to minimize the load shedding costs while maintaining radial topologies.

The remainder of the paper is organized as follows. Section II describes in detail the two-stage stochastic model for resilient planning of distribution systems and line damage modeling of extreme weather events. The simulation data are presented in Section III, and Section IV concludes the paper.

II. PROBLEM FORMULATION

Fig. 1 shows the framework proposed for improving the resilient planning of a distribution system. Prior to solving the SMILP model, the line outage uncertainty is modeled as a stochastic process. Afterward, a set of scenarios representing the realization of line outage uncertainty is generated. Then, in the first step, investment decisions such as DG installation and line hardening are made based on a certain budget. In the second step, dynamic microgrids are formed and then the system operation cost in term of optimal load shedding is minimized in each uncertain outage scenario. In fact, the post-event operational strategies are integrated into pre-event network planning for resilience improvement in both planning and operation steps. In the next step, the two-stage stochastic model is solved utilizing available software packages. The simulation results of the model assist the utilities to decide about hardening their distribution networks

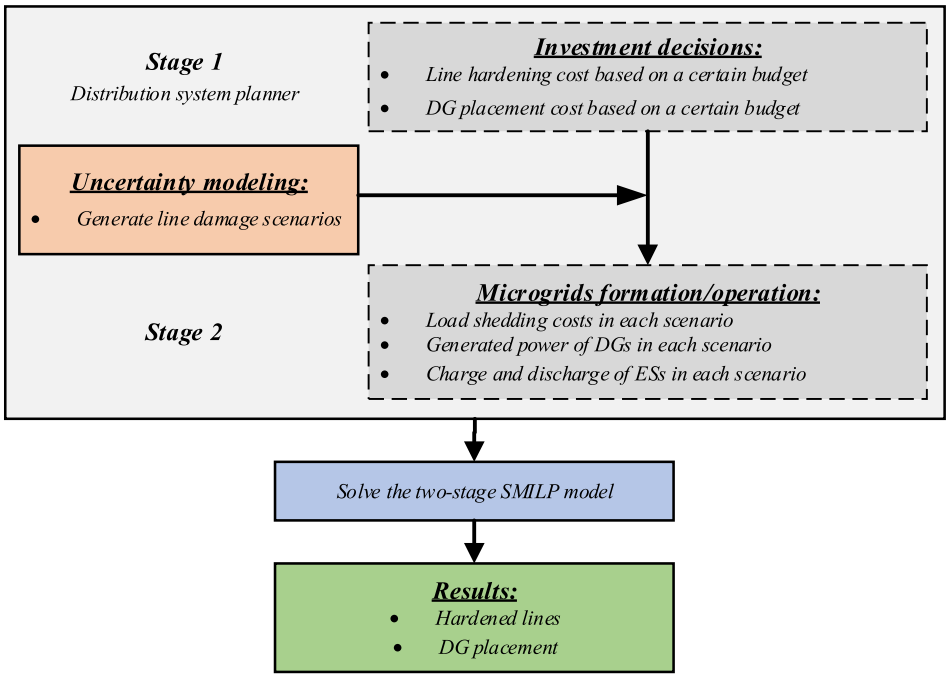

FIGURE 1. Framework for the resilient planning of a distribution system.

and allocating new back-up DGs with optimal investment and restoration costs.

In the following, the two-stage stochastic framework for the planning model under uncertainty is formulated; which consists of the first-stage problem considering DG allocation and line hardening in Section A; the second-stage problem considering microgrids formation, network reconfiguration, and distributed energy resources in Section B; and the uncertainty modeling in Section C.

A. DISTRIBUTION SYSTEM PLANNING MODEL

In this section, the objective function minimizes the investment cost in the first stage and the expectation of load shedding cost under line damage scenarios in the second stage, shown in (1). It is worth mentioning that the load shedding cost is used to assess the distribution system performance during extreme events, and this index has been widely utilized to evaluate the resilience of the distribution system [27], [28]. With a certain budget, a distribution system planner makes a scheme to allocate resources in order to improve the resilience of distribution systems. In this study, lines hardening and DG installation are considered as investment measures. Therefore, the budget constraint (2) indicates that the total investment cannot exceed a limited budget. Moreover, the binary variable $Z^{EM}_{m,b}$ is used to represent whether the DG m is installed at bus b in the planning stage. Constraint (3) shows that the bus inappropriate for DG allocation must be set to zero. Equation (4) represents that merely the DG allocated in the planning stage may be installed at the candidate bus. A maximum of one DG is located in each bus, as shown in constraint (5). Equation (6) indicates that each DG can be allocated to only one bus.

$$\min \sum_{l} c^{h}_{l} \times Y_{l} + \sum_{m} c^{dg} \times Z_{m} + \varphi_{h} \sum_{\omega} \rho_{\omega} \phi(\omega) \quad (1)$$

$$\sum_{l} c^{h}_{l} \times Y_{l} + \sum_{m} c^{dg} \times Z_{m} \leq B \quad (2)$$

$$Z^{EM}_{m,b} = 0, \quad \forall m, b \in \Omega_{NC} \quad (3)$$

$$Z^{EM}_{m,b} \leq Z_{m}, \quad \forall m, b \quad (4)$$

$$\sum_{m \in \Omega_{M}} Z^{EM}_{m,b'} \leq 1, \quad b' = \Omega_{B_{MDG}}(k) \quad (5)$$

$$\sum_{b'} Z^{EM}_{m,b'} \leq 1, \quad m = \Omega_{M} \quad (6)$$

B. OPERATIONAL STRATEGIES IN THE SECOND-STAGE

Under a given planning decision, the resilience of distribution systems is improved by post-event operational strategies of microgrid formation, network reconfiguration, and distributed energy resources. Particularly, the objective function of the second stage is to minimize the load shedding costs, as depicted in (7), and this equation has been used in the first-stage planning objective function.

$$\phi(\omega) = \min \sum_{k} \sum_{b} \sum_{t} c^{ls}_{b,t} \times (1 - \alpha_{b,k,\omega}) \times P_{b,t} \quad (7)$$

The network reconfiguration, microgrids formation and distributed energy resources are integrated into the distribution system planning model to increase the operational resilience. In addition, the strategy introduced in [29] is utilized for modeling a master-slave concept, which means that in each formatted microgrid, only one DG as a master

unit controls the voltage and frequency of the microgrid, and other DGs act as slave units. According to the above explanation, the topology and operational constraints are given as follows:

1) CONNECTION CONSTRAINT

Constraint (8) indicates that each bus of the network will only belong to either one of the formatted microgrids or none of them. Binary variable $\alpha_{b,k,\omega}$ defines that if the k-th of N_{MGs} is chosen as the master unit and bus b belongs to microgrid k, $\alpha_{b,k,\omega}$ will be 1 [17].

$$\sum_{k=1}^{N_{MGs}} \alpha_{b,k,\omega} \leq 1, \forall b, \omega \tag{8}$$

2) ROOT BUS CONSTRAINTS

Constraints (9) and (10) represent the root bus status. One can connect bus b in scenario ω to microgrid k only if the k-th member of the set $\Omega_{B_{MDG}}$ is selected as the root bus [17].

$$\alpha_{b,k,\omega} \leq \alpha_{b',k,\omega}, b' = \Omega_{B_{MDG}}(k), \quad \forall b, k, \omega \tag{9}$$

$$\alpha_{b',k,\omega} \leq \sum_{m \in \Omega_M} Z^{EM}_{m,b'}, b' = \Omega_{B_{MDG}}(k), \quad \forall \omega \tag{10}$$

3) BOUNDARY LINE CONSTRAINTS

If the two sides of a distribution line do not belong to the same microgrid during the formation of the microgrids, the binary variable indicating the line status must be set to zero, as shown in (11). Linear methods are used to transform this equation to the linear constraint. Hence, the equation (11) can be linearized using Eqs. (13)–(15) [5], [7].

$$\beta_{l,\omega} \leq \alpha_{b,k,\omega} \times \alpha_{b',k,\omega}, \quad \forall b, b', l, k, \omega \tag{11}$$

$$\beta_{l,\omega} = \sum_{k \in \Omega_K} \beta_{l,k,\omega}, \quad \forall l, \omega \tag{12}$$

$$\beta_{l,k,\omega} \leq \sum_{b} \alpha_{b,k,\omega}, b = \Omega_{IB}(l), \quad \forall l, k, \omega \tag{13}$$

$$\beta_{l,k,\omega} \leq \sum_{b'} \alpha_{b',k,\omega}, b' = \Omega_{TB}(l), \quad \forall l, k, \omega \tag{14}$$

$$\beta_{l,k,\omega} \geq \sum_{b} \alpha_{b,k,\omega} + \sum_{b'} \alpha_{b',k,\omega} - 1, \quad b = \Omega_{IB}(l), b' = \Omega_{TB}(l), \quad \forall l, k, \omega \tag{15}$$

4) LINE AND BUS STATUS CONSTRAINTS

Constraints (16)–(18) show the status of a line and a bus. The functional status of lines is connected using constraint (16) with their outage status and the line hardening variable decision. First, in the scenario generation stage, we should define $z_{l,\omega}$ for all lines. Subsequently, the active status of a line $\beta_{l,\omega}$ is defined according to the first-stage binary variable Y_l and the uncertainty realization. Constraints (17) and (18) are used for modeling the status of a distribution line and the damaged buses, respectively.

$$\beta_{l,\omega} \leq 1 - (1 - z_{l,\omega}) \times (1 - Y_l), \forall l, \omega \tag{16}$$

$$\alpha_{b,k,\omega} = \alpha_{b',k,\omega}, \quad b = \Omega_{IB}(l'), \quad b' = \Omega_{TB}(l'), \quad \forall l', HE_{l,\omega} \neq 0, k, \omega \tag{17}$$

$$\alpha_{b,k,\omega} \leq HB_{b,\omega}, \quad \forall b, k, \omega \tag{18}$$

5) RADIALITY CONSTRAINTS

In this part, the method described in [29] is used for modeling the radiality constraint in each microgrid. In the current approach, we create a fictitious network in which each formatted microgrid permits only a single energy source as a master control unit, while the other buses are sink buses with 1 p.u demand loads. According to [29], the connectivity constraints can be modeled by the following equations:

$$\sum_{b} \alpha_{b,k,\omega} \leq BM \times \lambda_{k,\omega}, \quad \forall k, \omega \tag{19}$$

$$\lambda_{k,\omega} \leq BM \times \sum_{b} \alpha_{b,k,\omega}, \quad \forall k, \omega \tag{20}$$

$$\sum_{l} \beta_{l,k,\omega} = \sum_{b} \alpha_{b,k,\omega} - \lambda_{k,\omega}, \quad \forall k, \omega \tag{21}$$

$$\sum_{b \in \Omega_{TB}} \sum_{l} \xi^{(1)}_{b,b',l,k,\omega} - \sum_{b \in \Omega_{IB}} \sum_{l} \xi^{(1)}_{b,b',l,k,\omega} = -\alpha_{b',k,\omega}, \quad b' \neq \Omega_{B_{MDG}}(k), \quad \forall k, \omega \tag{22}$$

$$\sum_{b \in \Omega_{TB}} \sum_{l} \xi^{(1)}_{b,b',l,k,\omega} - \sum_{b \in \Omega_{IB}} \sum_{l} \xi^{(1)}_{b,b',l,k,\omega} = -\xi^{(2)}_{b',k,\omega} \times \alpha_{b',k,\omega}, \quad b' = \Omega_{B_{MDG}}(k), \quad \forall k, \omega \tag{23}$$

$$-\beta_{l,k,\omega} \leq \xi^{(1)}_{b,b',l,k,\omega} \leq \beta_{l,k,\omega}, b \in \Omega_{TB}(l), \quad b' \in \Omega_{IB}(l), \quad \forall l, k, \omega \tag{24}$$

$$\alpha_{b',k,\omega} \leq \xi^{(2)}_{b',k,\omega} \leq BM \times \alpha_{b',k,\omega}, \quad b' = \Omega_{B_{MDG}}(k), \quad \forall k, \omega \tag{25}$$

6) LOAD DEMAND CONSTRAINTS

Here, we presume that the system operator is able to control some of the loads directly via utilizing the demand response contracts. Constraints (26) and (27) show the active power in every node with the load control capabilities in the second stage. According to constraint (28), if the load control is utilized to the active power of each load, the reactive power is decreased as well. In addition, the control capabilities of the loads are represented by Eqs. (29)–(31) [17].

$$p^{L}_{b,k,t,\omega} = \alpha_{b,k,\omega} \times P_{b,t}, \quad \forall b, k, t, \omega \tag{26}$$

$$p^{L}_{j,k,t,\omega} = \alpha_{j,k,\omega} \times P_{j,t} - p^{LC}_{j,k,t,\omega}, \quad \forall j, k, t, \omega \tag{27}$$

$$q^{L}_{b,k,t,\omega} = \alpha_{b,k,\omega} \times Q_{b,t} - tan(\varphi_b) \times p^{LC}_{b,k,t,\omega}, \quad \forall b, k, t, \omega \tag{28}$$

$$\sum_{k \in \Omega_K} p^{LC}_{j,k,t,\omega} = \sum_{d=1}^{D} \sigma^{L}_{j,d,t,\omega} \times p^{b}_{j,d,t,\omega}, \quad \forall j, t, \omega \tag{29}$$

$$p^{LC}_{j,k,t,\omega} \le \alpha_{j,k,\omega} \times DR^{L,Max}_{j,t}, \quad \forall j,k,t,\omega \tag{30}$$

$$\sum_{d=1}^{D} \sigma^{L}_{j,d,t,\omega} \le 1, \quad \forall j,t,\omega \tag{31}$$

7) DG CONSTRAINTS

Equations (32)–(35) show the active and reactive power limits of DGs if they have been allocated in the first stage. One can see that equation (32) represents a nonlinear constraint and must be converted to linear constraints. Hence, equation (32) may be linearized via constraints (36)–(38) [5].

$$\gamma_{b,k,\omega,m} = \alpha_{b,k,\omega} \times Z^{EM}_{m,b}, \quad \forall b,k,\omega,m \tag{32}$$

$$p^{DG}_{m,k,t,\omega} \le \sum_{b} \gamma_{b,k,\omega,m} \times P^{DG,Max}_{m}, \quad \forall m,k,t,\omega \tag{33}$$

$$q^{DG}_{m,k,t,\omega} \le \sum_{b} \gamma_{b,k,\omega,m} \times Q^{DG,Max}_{m}, \quad \forall m,k,t,\omega \tag{34}$$

$$q^{DG}_{m,k,t,\omega} \ge \sum_{b} \gamma_{b,k,\omega,m} \times Q^{DG,Min}_{m}, \quad \forall m,k,t,\omega \tag{35}$$

$$\gamma_{b,k,\omega,m} \le \alpha_{b,k,\omega}, \quad \forall b,m,k,\omega \tag{36}$$

$$\gamma_{b,k,\omega,m} \le Z^{EM}_{m,b}, \quad \forall b,m,k,\omega \tag{37}$$

$$\gamma_{b,k,\omega,m} \ge Z^{EM}_{m,b} + \alpha_{b,k,\omega} - 1, \quad \forall b,m,k,\omega \tag{38}$$

8) ENERGY STORAGES CONSTRAINTS

Constraints (39)–(42) depict the charging and discharging constraints of the energy storage (ES) units in the second stage. Moreover, equations (43)–(45) represent the limits of the maximum, minimum and initial charge levels of the energy storage units, respectively. The state of charge (SOC) of the storages at different time intervals is computed using equation (46) [7].

$$\gamma^{ES}_{e,k,t,\omega} \le \sum_{\Omega_E} \alpha_{b,k,\omega}, \quad \forall e,k,t,\omega \tag{39}$$

$$pes^{ch}_{e,k,t,\omega} \le \gamma^{ES}_{e,k,t,\omega} \times Rate^{ch,\max}_{e}, \quad \forall e,k,t,\omega \tag{40}$$

$$pes^{dch}_{e,k,t,\omega} \le (1-\gamma^{ES}_{e,k,t,\omega}) \times Rate^{dch,\max}_{e}, \quad \forall e,k,t,\omega \tag{41}$$

$$pes^{dch}_{e,k,t,\omega} \le \sum_{\Omega_E} \alpha_{i,k,\omega} \times Rate^{dch,\max}_{e}, \quad \forall e,k,t,\omega \tag{42}$$

$$soc^{ES}_{e,k,t,\omega} \le \sum_{\Omega_E} \alpha_{i,k,\omega} \times SOC^{ES,\max}_{e}, \quad \forall e,k,t,\omega \tag{43}$$

$$soc^{ES}_{e,k,t,\omega} \ge \sum_{\Omega_E} \alpha_{i,k,\omega} \times SOC^{ES,\min}_{e}, \quad \forall e,k,t,\omega \tag{44}$$

$$soc^{ES}_{e,k,t,\omega} = \sum_{\Omega_E} \alpha_{b,k,\omega} \times SOC^{ES,initial}_{e} + pes^{ch}_{e,k,t,\omega} \times \frac{\eta^{ES}_{e}}{Cap^{ES}_{e}} - pes^{dch}_{e,k,t,\omega} \times \frac{1}{\eta^{ES}_{e} \times Cap^{ES}_{e}}, \quad \forall e,k,t,\omega \tag{45}$$

$$soc^{ES}_{e,k,t,\omega} = soc^{ES}_{e,k-1,t,\omega} + pes^{ch}_{e,k,t,\omega} \times \frac{\eta^{ES}_{e}}{Cap^{ES}_{e}} - pes^{dch}_{e,k,t,\omega} \times \frac{1}{\eta^{ES}_{e} \times Cap^{ES}_{e}}, \quad \forall e,k,t,\omega \tag{46}$$

9) LINE FLOW CONSTRAINTS

Constraints (47) and (48) define the active and reactive power flows of the lines.

$$-\beta_{l,\omega} \times P^{Max}_{l} \le p_{l,t,\omega} \le \beta_{l,\omega} \times P^{Max}_{l}, \quad \forall l,t,\omega \tag{47}$$

$$-\beta_{l,\omega} \times Q^{Max}_{l} \le q_{l,t,\omega} \le \beta_{l,\omega} \times Q^{Max}_{l}, \quad \forall l,t,\omega \tag{48}$$

10) POWER BALANCE IN EACH BUS

The active and reactive power balances in each node are illustrated in (49) and (53). Due to the use of bilinear terms $P^{DG}_{m,k,t,\omega} \cdot Z^{EM}_{m,b}$ in (49) and $Q^{DG}_{m,k,t,\omega} \cdot Z^{EM}_{m,b}$ in (53), these constraints are nonlinear. Therefore, constraints (50)–(52) and (54)–(56) are used to transform the nonlinear constraints [17].

$$\sum_{\forall k \in \Omega_K} \left[\sum_{\forall m} p^{DG,dep}_{m,b,k,t,\omega} - p^{L}_{b,k,t,\omega} \right] = \sum_{l \in \Omega_l} -p_{l,t,\omega} \times MapTL_{b,l}, \quad \forall b,t,\omega \tag{49}$$

$$p^{DG,dep}_{m,b,k,t,\omega} \le P^{DG,Max}_{m} \times Z^{EM}_{m,b}, \quad \forall m,b,k,t,\omega \tag{50}$$

$$p^{DG,dep}_{m,b,k,t,\omega} \le p^{DG}_{m,k,t,\omega}, \quad \forall m,b,k,t,\omega \tag{51}$$

$$p^{DG,dep}_{m,b,k,t,\omega} \ge p^{DG}_{m,k,t,\omega} - P^{DG,Max}_{m} \times (1 - Z^{EM}_{m,b}), \quad \forall m,b,k,t,\omega \tag{52}$$

$$\sum_{\forall k \in \Omega_K} \left[\sum_{\forall m} q^{DG,dep}_{m,b,k,t,\omega} - q^{l}_{b,k,t,\omega} \right] = \sum_{l \in \Omega_l} -q_{l,t,\omega} \times MapTL_{b,k}, \quad \forall b,t,\omega \tag{53}$$

$$q^{DG,dep}_{m,b,k,t,\omega} \le Q^{DG,Max}_{m} \times Z^{EM}_{m,b}, \quad \forall m,b,k,t,\omega \tag{54}$$

$$q^{DG,dep}_{m,b,k,t,\omega} \le q^{DG}_{m,k,t,\omega}, \quad \forall m,b,k,t,\omega \tag{55}$$

$$q^{DG,dep}_{m,b,k,t,\omega} \ge q^{DG}_{m,k,t,\omega} - Q^{DG,Max}_{m} \times (1 - Z^{EM}_{m,b}), \quad \forall m,b,k,t,\omega \tag{56}$$

11) BUS VOLTAGE CONSTRAINTS

Magnitude and angles constraints on the node voltages are defined using (57) and (58). The voltage magnitude of master unit k is set to the controlled value (1 p.u), as shown in constraint (59). Besides, constraint (60) forces its voltage angle to be zero [17].

$$\alpha_{b,k,\omega} \times V^{min} \le v_{b,k,t,\omega} \le \alpha_{b,k,\omega} \times V^{max}, \quad \forall b,k,t,\omega \tag{57}$$

$$-\alpha_{b,k,\omega} \times \delta^{max} \le \delta_{b,k,t,\omega} \le \alpha_{b,k,\omega} \times \delta^{max}, \quad \forall b,k,t,\omega \tag{58}$$

$$v_{b,k,t,\omega} = \alpha_{b,k,\omega} \times V^{DG,set}_{k}, \quad \forall b \in \Omega_{B_{MDG}}, \quad \forall k,t,\omega \tag{59}$$

$$-\left(1-\alpha_{b,k,\omega}\right) \times \delta^{max} \le \delta_{b,k,t,\omega} \le \left(1-\alpha_{b,k}\right) \times \delta^{max}, \quad \forall b \in \Omega_{B_{MDG}}, \quad \forall k,t,\omega \tag{60}$$

12) LOAD FLOW LIMITS

In this section, the method presented in [17] is utilized to perform load flow computations in the distribution network.

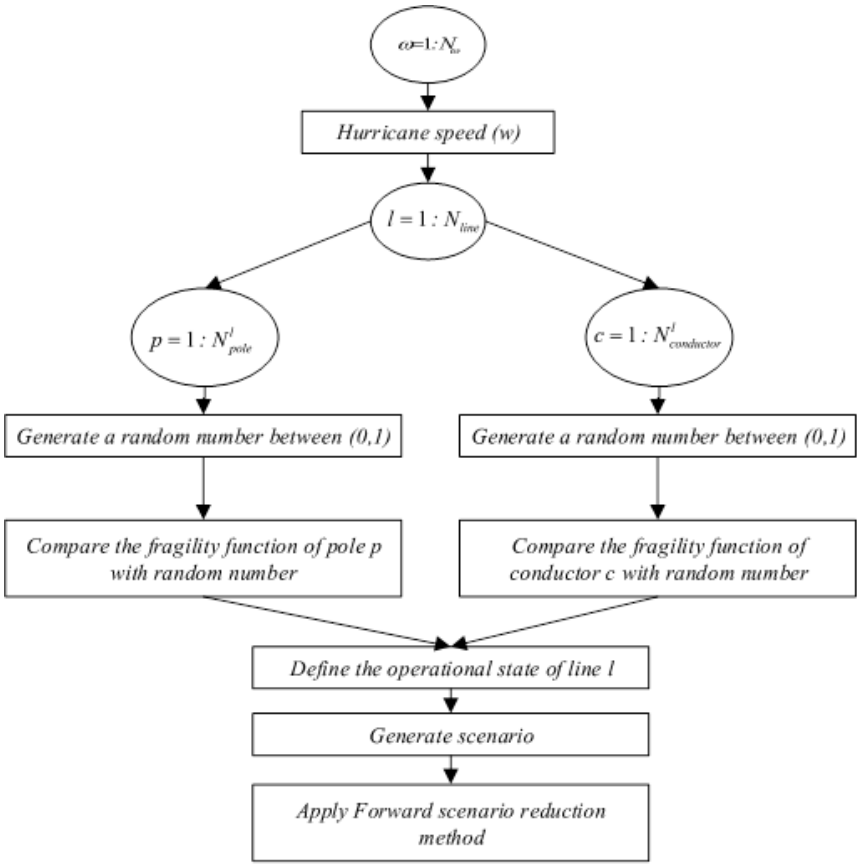

FIGURE 2. Flowchart of line damage scenario generation.

Using this approach, the node voltage magnitudes and angles are computed according to a suitable linear approximation. Constraints (61)–(63) define the linearized load flow equations. Moreover, the slack variable restrictions are shown in equations (64)–(66) for validating equality constraints when the two buses of one line are not in the same microgrid.

$$E1_l = \frac{r_l}{r_l^2+x_l^2}, \quad E2_l = \frac{x_l}{r_l^2+x_l^2} \tag{61}$$

$$p_{l,t,\omega} = zp_{l,t,\omega} + \sum_k \left[\delta_{b,k,t,\omega} - \delta_{r,k,t,\omega}\right] \times E2_l + \sum_k \left[v_{b,k,t,\omega} - v_{b',k,t,\omega}\right] \times E1_l, \ \forall l, t, \omega \tag{62}$$

$$q_{l,t,\omega} = zq_{l,t,\omega} + \sum_k \left[\delta_{b,k,t,\omega} - \delta_{b',k,t,\omega}\right] \times E1_l + \sum_k \left[v_{b,k,t,\omega} - v_{b',k,t,\omega}\right] \times E2_l, \quad \forall l, t, \omega \tag{63}$$

$$-\left(1-\beta_{l,\omega}\right) \times BM \le zp_{l,t,\omega} + \varepsilon \le \left(1-\beta_{l,\omega}\right) \times BM, \quad \forall l, t, \omega \tag{64}$$

$$-\left(1-\beta_{l,\omega}\right) \times BM \le zq_{l,t,\omega} + \varepsilon \le \left(1-\beta_{l,\omega}\right) \times BM, \quad \forall l, t, \omega \tag{65}$$

$$-0.01 \le \varepsilon \le 0.01 \tag{66}$$

C. LINE DAMAGE SCENARIOS GENERATION

In this paper, the operational status of distribution lines against hurricanes are considered uncertain set. The process of line outage scenario generation is shown in Fig. 2. In distribution networks, overhead distribution lines (conductors) and poles can be damaged by hurricanes. The fragility function of conductors and poles is given as follows [30]–[32]:

$$p_{pole}(w) = \left\{0.0001e^{0.0421w}, 1\right\} \tag{67}$$

$$p_{cond}(w) = \begin{cases} 0, & \mathrm{w} \le \mathrm{w}_{\min} \\ \frac{w-w_{\min}}{w_{\max}-w_{\min}}, & \mathrm{w}_{\min} \le \mathrm{w} \le \mathrm{w}_{\max} \\ 1, & \mathrm{w} \ge \mathrm{w}_{\max} \end{cases} \tag{68}$$

In the scenario generation phase, one must investigate the hurricane occurrence model in the distribution system. Therefore, in the present paper, we consider hurricanes in categories 1-3. Moreover, it is considered that the hurricane happens with various speeds in each scenario based on the probability of each hurricane category. Then, for each scenario, the operational status of the conductors and poles of each distribution line is extracted by comparing the failure probability, which is computed through the fragility functions and the random number sampling from the uniform distribution (0, 1). Hence, the operational status of each line is defined. It is worth mentioning that a distribution line is failed if the conductor or any distribution pole between the

TABLE 2. Cost of strategies to enhance resilience.

Strategy	Cost ($)
Upgrading pole	6000/pole [34]
Installing a natural gas-fired CHPs as DG	1000/kW [25]

associate nodes is failed. In addition, we presume that failure probabilities of poles are independent and all poles have the same fragility function. However, a few resilience researches consider the fact that the joint failure probabilities of multiple lines can be modeled [33].

III. CASE STUDY AND NUMERICAL RESULTS

In this section, a modified IEEE 33-bus distribution system and IEEE 69-bus distribution system are utilized for validating the effectiveness of the proposed SMILP model. It is assumed that average occurrences of hurricanes in a year are one. The duration of the failure state is considered to be 15 hours (between 10:00 and 24:00). Table 2 shows the initial investment costs of the two considered resilience improvement options. The length of each distribution line is presumed to be proportional to its resistance. Hence, we can calculate the number of distribution poles in every distribution line. It is assumed that the distance between two consecutive poles is 150 ft. Also, the resilience improvement options are assumed to have a life time of 15 years. Considering a 10% interest rate, the annual investment cost for the purchase and installation of each option is a tenth of the original investment cost. The penalty cost for load shedding is considered to be 14 $/kWh [11], and the load shedding cost parameter is the product of the load priority and the load shedding penalty cost. The assumed multipliers of the load profile are shown in Fig. 3 [35]. Also, we consider the same multipliers for all the buses. The lower and upper limits of the voltage range are set to 0.9 and 1.1 pu, respectively. The proposed model was implemented using GAMS environment and solved using CPLEX solver with a 0.01% optimality gap. Our simulation is done on a PC with a 3.2-GHz Intel Core i7 processor and 32 GB of RAM. The computation time is 30-60 minutes for the IEEE 33-bus distribution system and approximately 2 hours for the IEEE 69-bus distribution system.

A. IEEE 33-BUS DISTRIBUTION SYSTEM

This case study has six normally-closed lines, five tie lines, and one upstream substation. It is assumed that controllable back-up DGs with 1000-kW capacities are used by utilities

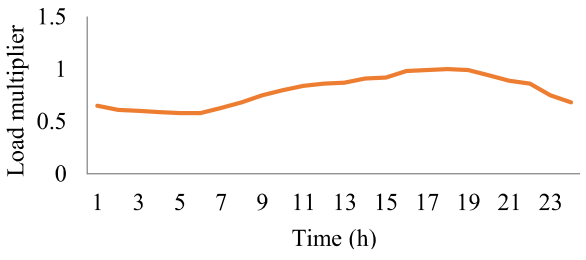

FIGURE 3. Load profile multiplier.

for boosting the network resilience. The buses 11, 21, 24, 25, and 30 are selected as candidates for the natural gas-fired DG installation as master units. Nodes 4, 7, 8, 14, 24, 25, 29, 30, 31, and 32 are demand-response-capable. These nodes can only apply load shedding. The blocks of the load control are considered to be 100 kW, and the controlling options have five levels. In the last level, if the load reduces below 100 kW, the load will be interrupted entirely. There are two energy storage units, which are installed on nodes 22 and 33. The capacity, charging and discharging rates, initial SOC, and efficiency of the energy storage units are considered to be 100 kWh, 50 kW, 60% and 0.85, respectively. The detailed bus and distribution line data are available in [36].

1) CASE 1: EFFECTIVENESS OF MICROGRID FORMATION STRATEGY

Here, the effects of the microgrid formation on the resilience of a distribution system during the failure state when the upstream network is available have been studied. A demonstration case considering three scenarios for the distribution line outage status is used to illustrate the effectiveness of the presented model. The optimal planning measures and the scenarios of line outages with reconfiguration are shown in Fig. 4.

In the planning stage with a $ 250,000 hardening budget, two DGs are installed, and four lines are hardened according to the proposed distribution system planning model. With the realization of line outage uncertainty, specific distribution lines are damaged in three scenarios as depicted in Fig. 4 (a)–(c). In each scenario, the planning decisions are adopted and the operational strategies of microgrid formation, network reconfiguration, and demand-side management are employed to restore critical loads in the emergency response stage.

For instance, distribution lines 7-8, 12-13, 16-17, and 19-20 are damaged in Fig. 4 (a). In this case, line 19-20 is hardened and two DGs are installed in candidate nodes 11 and 30 to restore loads in a critical situation. Moreover, the tie-lines 18-33 and 25-29 are closed, and the normally-closed lines 3-23, 6-26, and 15-16 are opened to form three microgrids with the main grid, DG1 and DG2, respectively. Similar analyses can be carried out for other scenarios.

Table 3 displays the simulation results of the 33-bus system with and without microgrid formation strategy. Moreover, In Fig. 5, the investment decisions without the microgrid formation strategy are shown. It is worth mentioning that, in Fig. 5, without microgrid formation strategy means that the distribution network has not used the normally closed lines.

As depicted in Table 3, the load shedding increases without the utilization of the microgrid formation strategy. The reason is the disconnection of the distribution network from the upstream network to supply loads. In addition, without the utilization of the normally closed lines, the distribution system cannot sectionalize itself into multiple microgrids to recover the critical loads during disasters. In fact, one master

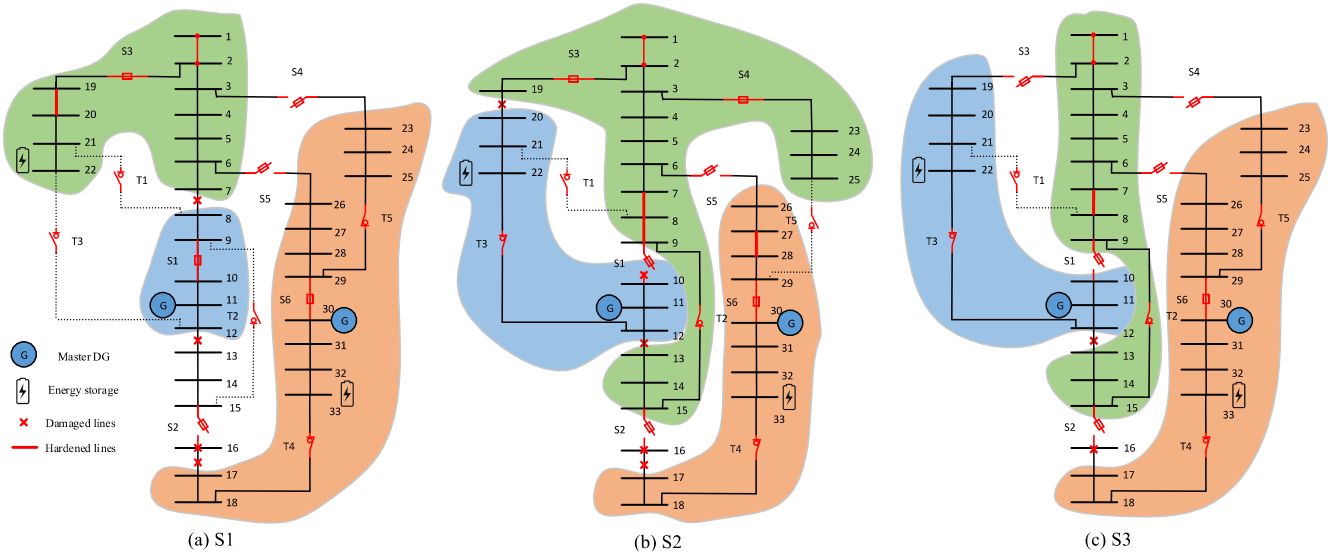

FIGURE 4. Optimal planning results for the 33-bus test system.

TABLE 3. Simulation results of the 33-bus distribution network.

	Without microgrid formation strategy	With microgrid formation strategy
Total investment cost ($)	100,000	241,400
Line hardening cost ($)	-	41,400
Total load shedding cost ($)	1,153,516.59	424,159.78

DG is installed in node 11, and only one microgrid is formed due to not using the normally closed lines. Thus, adopting the microgrid formation approach can considerably decrease the load shedding cost more than %63. On the other hand, considering the microgrid formation strategy can enhance the distribution system flexibility in the recovery phase.

2) CASE 2: EFFECTIVENESS OF NETWORK RECONFIGURATION

This section is designed to illustrate the effectiveness of the network reconfiguration on resilient distribution system planning against hurricane. The location of DGs and the hardened lines and the configuration of distribution network without tie-lines are shown Fig. 6(a)–(c). It should be mentioned that ''without reconfiguration'' means that the distribution network is in its initial configuration. In this case, the line hardening cost and the cost of loss of load are $4 9,200 and $ 441,413.59, respectively.

As shown in these figures, considering tie-lines as an operational strategy can significantly decrease the investment cost, especially the line hardening cost. In fact, in comparison with Section III-A, the load shedding and line hardening costs increased approximately %15 and %3.9, respectively. As a consequence, the combination of the planning and operational actions such as microgrid formation and network reconfiguration can efficiently enhance the resilience of distribution systems.

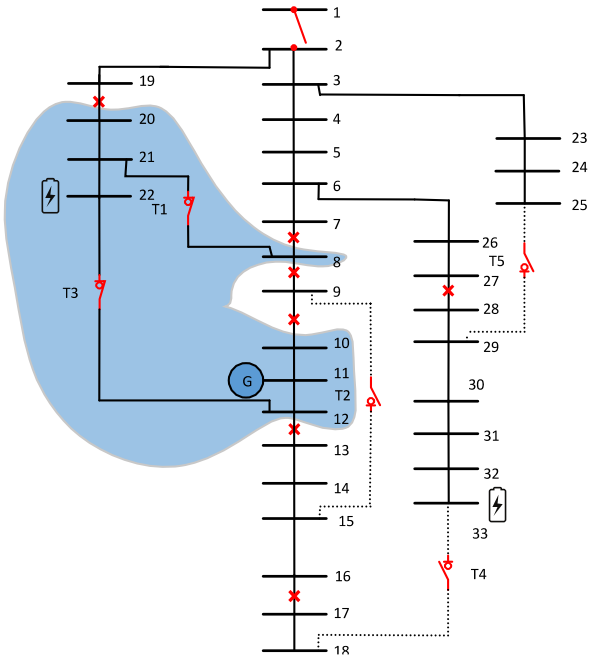

FIGURE 5. Optimal planning results without microgrid formation strategy.

3) CASE 3: EFFECT OF THE HARDENING BUDGET

This section investigates the dynamic microgrid formation and load shedding cost with various hardening budgets from $B = 0$ to $B = 300{,}000$ to validate the effectiveness of the hardening budget. The investment cost and the total cost associated with load shedding are shown in Table 4. In the absence of the hardening budget, the line outage uncertainty will impose $ 734,440.73 in the network load shedding cost. If we increase the hardening budget to $ 50,000, the loss of load cost will be reduced to $ 628,425.68. However, the cost of loss of load will not always lessen as we increase the hardening budget.

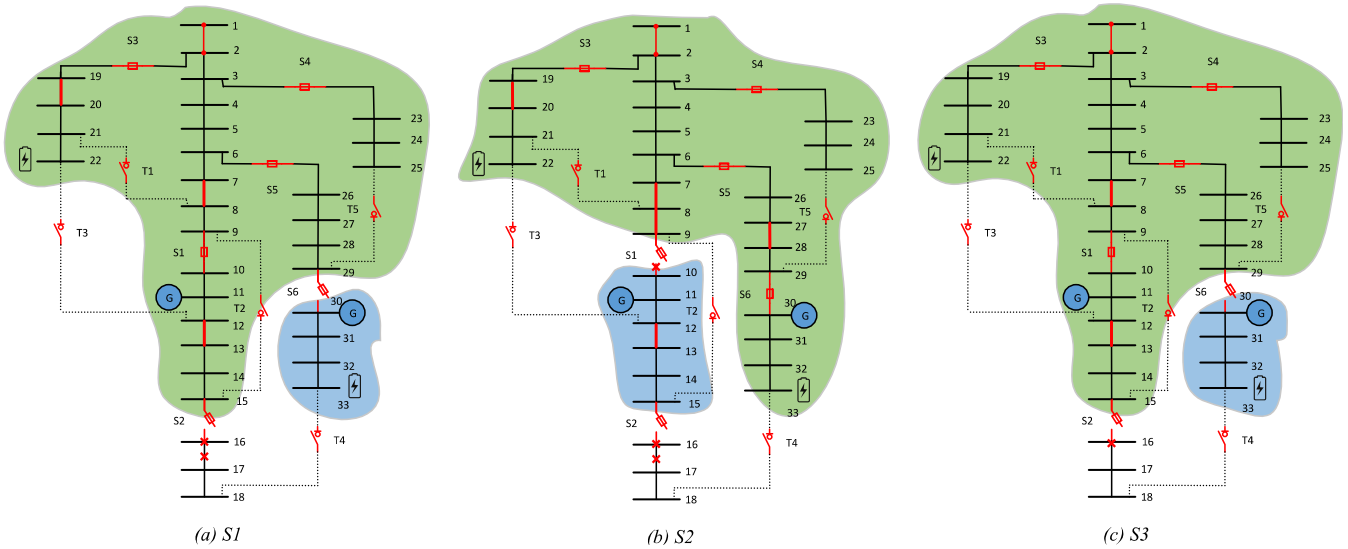

FIGURE 6. Optimal planning results without network reconfiguration.

TABLE 4. Planning results for the 33-bus test system under different hardening budgets.

B	Investment cost ($)	Load shedding Cost ($)
0	0	734,440.73
50,000	33,600	628,425.68
100,000	100,000	582,032.11
150,000	141,400	474,675.09
200,000	141,400	474,675.09
250,000	241,400	424,159.78
300,000	256,400	417,258.26

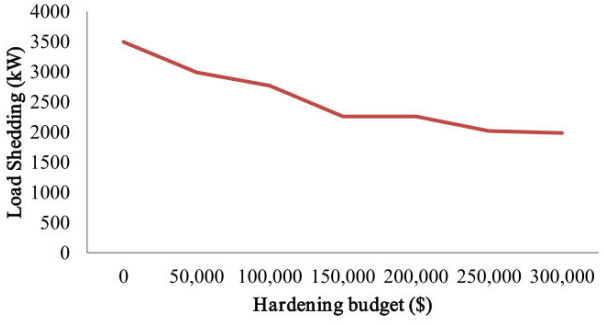

FIGURE 7. The load shedding under different hardening budgets.

The reason is that hardened lines (with fixed numbers of DGs) cannot alter the microgrid formation. In Table 4, when $B = 150{,}000$ and 200,000, the hardening plans are the same, e.g., the four distribution lines 7-8, 8-9, 19-20, and 27-28 are hardened. With a hardening budget of $ 300,000, the loss of load cost will drop from $ 734,440.73 to $ 417,258.26, a decrease of more than % 43. This illustrates the effectiveness of DG placement and distribution line hardening. Moreover, the load shedding for the IEEE 33-bus distribution network is shown in Fig. 7.

Obviously, the investment schemes offer an effective plan for the determination of the distribution hardening budget via a comparison of the marginal benefits.

B. IEEE 69-BUS DISTRIBUTION SYSTEM

This test network involves a 12.66 kV distribution system with 1 medium voltage feeder, 69 nodes, 71 lines, 3 tie lines, and 8 normally-closed lines. The total active and reactive power demands of this system are 3.8 MW and 2.69 Mvar, respectively. The distribution system contains 1200-kW back-up DGs. The newly installed DGs are restricted to a total number of two. The candidate positions for DG placement are 11, 21, 30, 50, and 61. Nodes 11, 12, 21, 49, 50, 61, and 64 are considered as demand-response-capable. Similar to the 33-bus system, the load control blocks are considered to be 100 kW, and the controlling options have five levels. There are two energy storage units, which are installed on nodes 17 and 37. The characteristics of the energy storage units are similar to the 33-bus system. In [37] and [38], the accurate data of the distribution system loads and line parameters are given.

According to the proposed distribution system planning model, two DGs are installed, and nine distribution lines are hardened considering a $ 300,000 hardening budget. In this state, the investment cost in the 69-bus distribution system is $ 299,400. Fig. 8 illustrates the optimal planning decisions resulting from solving the proposed method for scenarios when the distribution system is connecting to the upstream network. In Fig. 8(a)–(c), there were 7, 15, and 3 faulty lines isolated via the normally-closed lines in scenario S1, S2, and S3, respectively. As shown in this figure, the distribution system sectionalized itself into multiple microgrids. For example, two DGs are installed in line damage scenarios. Moreover, 2, 8, and 1 faulty line are hardened to form multiple microgrids for reducing the load shedding cost in

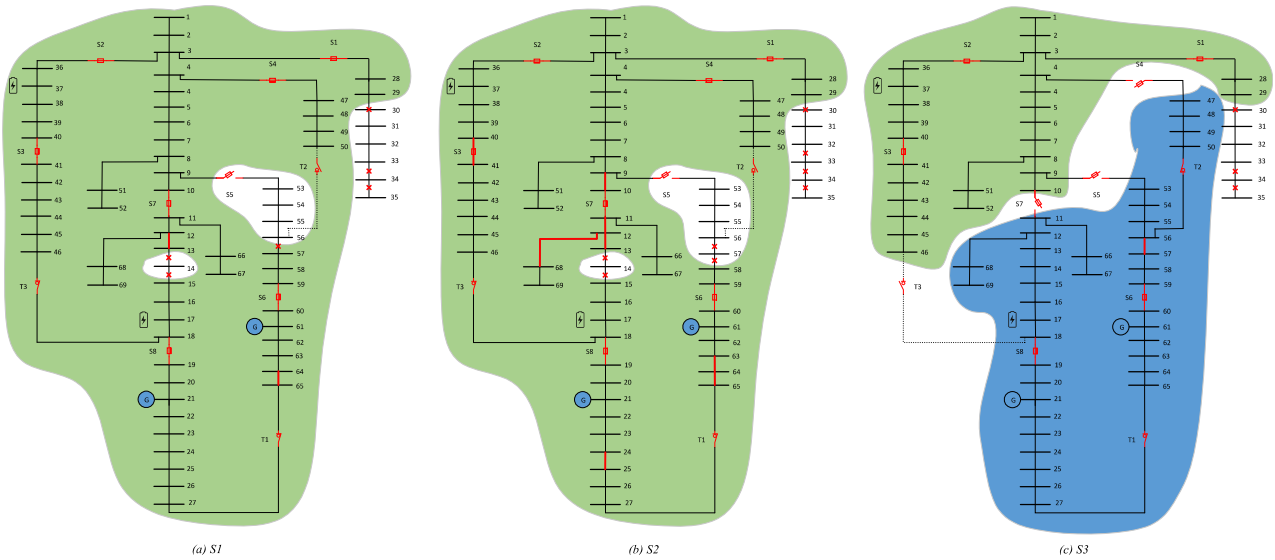

FIGURE 8. Optimal planning schemes of scenario S1-S3 in the 69-node system.

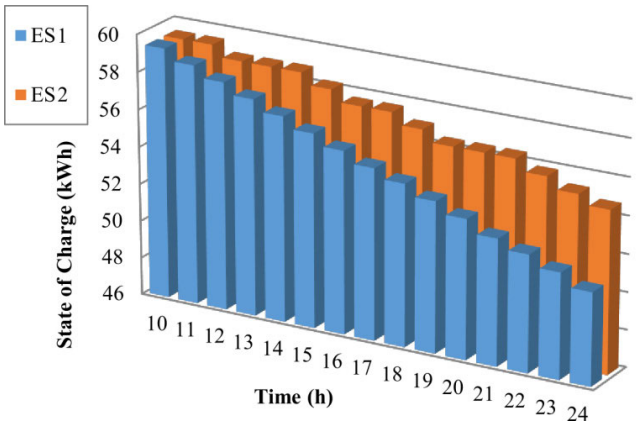

FIGURE 9. The average SOC level of the energy storage units during a hurricane.

scenario S1, S2, and S3, respectively. These simulation results depict that the presented model can form microgrids through master-slave control technique and network reconfiguration for restoring the critical loads. In Table 5, the load shedding cost under 3 different scenarios for the cases B = 0 and B = 300,000 are provided. It can be seen that the cost of load shedding with $ 300,000 hardening budget is significantly smaller than the state without investment plans in the presence of the upstream network. As shown in this table, the load shedding cost reduction in the IEEE 69-bus distribution network is approximately %36. In fact, it mean that the optimal investment schemes can directly reduce the economic losses during disasters.

Moreover, the average SOC level of the energy storage units is depicted in Fig. 9. Based on the results, the two energy storage units are fully operated and the maximum capacity of them is utilized to supply loads during disaster. In addition, the SOC levels of the two energy storage units are decreased at the end of the scheduled period.

TABLE 5. Planning results for the 69-node test system.

Scenarios	Load shedding cost ($)	
	B=0	B=300,000
S_1	815,890.1	529,655.22
S_2	893,016.51	529,655.22
S_3	759,713.76	519,947.6
Totally	2,468,620.37	1,579,258.04

IV. CONCLUSION

In this study, we proposed a novel model for the resilient distribution system planning with line hardening and DG placement based on two-stage stochastic optimization to minimize the load shedding costs against natural disasters. To do this optimally, the master-slave control method was used to coordinate resources within each microgrid in the second stage. Moreover, we applied load control blocks and energy storage units to help the system operator in improving distribution system performance in the restoration stage. It was demonstrated that the combination of planning and operational strategies can significantly increase the resilience of distribution systems. According to the simulation results, the use of the microgrid formation strategy and network reconfiguration can significantly reduce load shedding costs by %63 during hurricanes. In addition, the hardening cost increases by ∼%15 without considering network reconfiguration. However, as has been shown in the case study, determining a proper hardening budget can efficiently decrease the cost of loss of loads. In future works, we will study the impact of line damage and load uncertainties on the microgrid formation strategy in the resilient planning model.

REFERENCES

[1] P. H. Larsen, M. Lawson, K. H. LaCommare, and J. H. Eto, "Severe weather, utility spending, and the long-term reliability of the U.S. power system," *Energy*, vol. 198, May 2020, Art. no. 117387.

[2] E. B. Watson and A. H. Etemadi, "Modeling electrical grid resilience under hurricane wind conditions with increased solar and wind power generation," *IEEE Trans. Power Syst.*, vol. 35, no. 2, pp. 929–937, Mar. 2020.
[3] M. Sadeghi Khomami, M. Tourandaz Kenari, and M. S. Sepasian, "A warning indicator for distribution network to extreme weather events," *Int. Trans. Electr. Energy Syst.*, vol. 29, no. 8, Aug. 2019, Art. no. e12027.
[4] J. Najafi, A. Peiravi, and A. Anvari-Moghaddam, "Enhancing integrated power and water distribution networks seismic resilience leveraging microgrids," *Sustainability*, vol. 12, no. 6, p. 2167, Mar. 2020.
[5] X. Wang, Z. Li, M. Shahidehpour, and C. Jiang, "Robust line hardening strategies for improving the resilience of distribution systems with variable renewable resources," *IEEE Trans. Sustain. Energy*, vol. 10, no. 1, pp. 386–395, Dec. 2017.
[6] Y. Lin and Z. Bie, "Tri-level optimal hardening plan for a resilient distribution system considering reconfiguration and DG islanding," *Appl. Energy*, vol. 210, pp. 1266–1279, Jan. 2018.
[7] M. A. Gilani, A. Kazemi, and M. Ghasemi, "Distribution system resilience enhancement by microgrid formation considering distributed energy resources," *Energy*, vol. 191, Jan. 2020, Art. no. 116442.
[8] A. Younesi, H. Shayeghi, P. Siano, A. Safari, and H. H. Alhelou, "Enhancing the resilience of operational microgrids through a two-stage scheduling strategy considering the impact of uncertainties," *IEEE Access*, vol. 21, no. 9, pp. 18454–18464, Jan. 2021.
[9] M. Salimi, M.-A. Nasr, S. H. Hosseinian, G. B. Gharehpetian, and M. Shahidehpour, "Information gap decision theory-based active distribution system planning for resilience enhancement," *IEEE Trans. Smart Grid*, vol. 11, no. 5, pp. 4390–4402, Sep. 2020.
[10] A. H. M. Aldarajee, S. H. Hosseinian, B. Vahidi, and S. Dehghan, "A coordinated planner-disaster-risk-averse-planner investment model for enhancing the resilience of integrated electric power and natural gas networks," *Int. J. Electr. Power Energy Syst.*, vol. 119, Jul. 2020, Art. no. 105948.
[11] G. Zhang, F. Zhang, X. Zhang, Q. Wu, and K. Meng, "A multi-disaster-scenario distributionally robust planning model for enhancing the resilience of distribution systems," *Int. J. Electr. Power Energy Syst.*, vol. 122, Nov. 2020, Art. no. 106161.
[12] H. Wang, S. Wang, L. Yu, and P. Hu, "A novel planning-attack-reconfiguration method for enhancing resilience of distribution systems considering the whole process of resiliency," *Int. Trans. Electr. Energy Syst.*, vol. 30, no. 2, p. 12199, Feb. 2020.
[13] B. Chen, "Applications of optimization under uncertainty methods on power system planning problems," Ph.D. dissertation, Dep. Ind. Eng., Iowa State Univ., Ames, IA, USA, 2016.
[14] S. Ma, L. Su, Z. Wang, F. Qiu, and G. Guo, "Resilience enhancement of distribution grids against extreme weather events," *IEEE Trans. Power Syst.*, vol. 33, no. 5, pp. 4842–4853, Apr. 2018.
[15] E. Yamangil, R. Bent, and S. Backhaus, "Resilient upgrade of electrical distribution grids," in *Proc. 29th AAAI Conf. Artif. Intell.*, 2015, pp. 1233–1240.
[16] Q. Shi, F. Li, T. Kuruganti, M. Olama, J. Dong, X. Wang, and C. Winstead, "Resilience-oriented DG siting and sizing considering stochastic scenario reduction," *IEEE Trans. Power Syst.*, early access, Dec. 18, 2020, doi: 10.1109/TPWRS.2020.3043874.
[17] M. Ghasemi, A. Kazemi, A. Mazza, and E. Bompard, "A three-stage stochastic planning model for enhancing the resilience of distribution systems with microgrid formation strategy," *IET Gener., Transmiss. Distrib.*, Feb. 2021, doi: 10.1049/gtd2.12144.
[18] K. Kopsidas and M. Abogaleela, "Utilizing demand response to improve network reliability and ageing resilience," *IEEE Trans. Power Syst.*, vol. 34, no. 3, pp. 2216–2227, May 2019.
[19] T. Khalili, A. Bidram, and M. J. Reno, "Impact study of demand response program on the resilience of dynamic clustered distribution systems," *IET Gener., Transmiss. Distrib.*, vol. 14, no. 22, pp. 5230–5238, Nov. 2020.
[20] S. Nikkhah, K. Jalilpoor, E. Kianmehr, and G. B. Gharehpetian, "Optimal wind turbine allocation and network reconfiguration for enhancing resiliency of system after major faults caused by natural disaster considering uncertainty," *IET Renew. Power Gener.*, vol. 12, no. 12, pp. 1413–1423, Jul. 2018.
[21] M. S. Khomami, K. Jalilpoor, M. T. Kenari, and M. S. Sepasian, "Bi-level network reconfiguration model to improve the resilience of distribution systems against extreme weather events," *IET Gener., Transmiss. Distrib.*, vol. 13, no. 15, pp. 3302–3310, May 2019.
[22] J. Najafi, A. Peiravi, A. Anvari-Moghaddam, and J. M. Guerrero, "Resilience improvement planning of power-water distribution systems with multiple microgrids against hurricanes using clean strategies," *J. Clean. Production*, vol. 223, pp. 109–126, Jun. 2019.
[23] J. Kim and Y. Dvorkin, "Enhancing distribution system resilience with mobile energy storage and microgrids," *IEEE Trans. Smart Grid*, vol. 10, no. 5, pp. 4996–5006, Sep. 2019.
[24] S. Lei, J. Wang, C. Chen, and Y. Hou, "Mobile emergency generator pre-positioning and real-time allocation for resilient response to natural disasters," *IEEE Trans. Smart Grid*, vol. 9, no. 3, pp. 2030–2041, Sep. 2016.
[25] S. Ma, S. Li, Z. Wang, and F. Qiu, "Resilience-oriented design of distribution systems," *IEEE Trans. Power Syst.*, vol. 34, no. 4, pp. 2880–2891, Jan. 2019.
[26] J. Najafi, A. Peiravi, and J. M. Guerrero, "Power distribution system improvement planning under hurricanes based on a new resilience index," *Sustain. Cities Soc.*, vol. 39, pp. 592–604, May 2018.
[27] G. Wang, "Integration of preventive and emergency responses to boost distribution system resilience against windstorms," Ph.D. dissertation, Dept. Eng., Univ. Wisconsin-Milwaukee, Milwaukee, WI, USA, 2019.
[28] S. Ma, B. Chen, and Z. Wang, "Resilience enhancement strategy for distribution systems under extreme weather events," *IEEE Trans. Smart Grid*, vol. 9, no. 2, pp. 1442–1451, Jul. 2016.
[29] T. Ding, Y. Lin, Z. Bie, and C. Chen, "A resilient microgrid formation strategy for load restoration considering master-slave distributed generators and topology reconfiguration," *Appl. Energy*, vol. 199, pp. 205–216, Aug. 2017.
[30] A. M. Salman, Y. Li, and M. G. Stewart, "Evaluating system reliability and targeted hardening strategies of power distribution systems subjected to hurricanes," *Rel. Eng. Syst. Saf.*, vol. 144, pp. 319–333, Dec. 2015.
[31] M. Ghasemi, A. Kazemi, R. Dashti, M. A. Rajabi, and M. A. Gilani, "Resilience evaluation and prediction in electrical distribution systems: A case study in golestan province," in *Proc. 24th Electr. Power Distrib. Conf. (EPDC)*, Jun. 2019, pp. 6–9.
[32] J. Najafi, A. Peiravi, A. Anvari-Moghaddam, and J. M. Guerrero, "An efficient interactive framework for improving resilience of power-water distribution systems with multiple privately-owned microgrids," *Int. J. Electr. Power Energy Syst.*, vol. 116, Mar. 2020, Art. no. 105550.
[33] B. Vass, J. Tapolcai, Z. Heszberger, J. Biro, D. Hay, F. A. Kuipers, J. Oostenbrink, A. Valentini, and L. Ronyai, "Probabilistic shared risk link groups modeling correlated resource failures caused by disasters," *IEEE J. Sel. Areas Commun.*, early access, Mar. 9, 2021, doi: 10.1109/JSAC.2021.3064652.
[34] A. Shahbazi, J. Aghaei, S. Pirouzi, M. Shafie-khah, and J. P. S. Catalão, "Hybrid stochastic/robust optimization model for resilient architecture of distribution networks against extreme weather conditions," *Int. J. Electr. Power Energy Syst.*, vol. 126, Mar. 2021, Art. no. 106576.
[35] Z. Wang, B. Chen, J. Wang, and C. Chen, "Networked microgrids for self-healing power systems," *IEEE Trans. Smart Grid*, vol. 7, no. 1, pp. 310–319, Jun. 2015.
[36] A. Abessi, S. Jadid, and M. M. A. Salama, "A new model for a resilient distribution system after natural disasters using microgrid formation and considering ICE cars," *IEEE Access*, vol. 9, pp. 4616–4629, 2021.
[37] J. Shukla, B. K. Panigrahi, and P. K. Ray, "Stochastic reconfiguration of distribution system considering stability, correlated loads and renewable energy based DGs with varying penetration," *Sustain. Energy, Grids Netw.*, vol. 23, no. 23, Sep. 2020, Art. no. 100366.
[38] K. P. Swain and M. De, "A novel electrical proximity index for voltage control in smart distribution system," *Electr. Power Syst. Res.*, vol. 172, pp. 50–62, Jul. 2019.

MOSTAFA GHASEMI received the B.S. degree in electrical engineering from the Babol Noshirvani University of Technology, in 2013, and the M.S. degree in power system from the Iran University of Science and Technology, Iran, in 2016, where he is currently pursuing the Ph.D. degree in electrical engineering. His research interests include operation and planning of power systems, smart grids, and distribution system resilience.

AHAD KAZEMI received the M.Sc. degree in electrical engineering from Oklahoma State University, Stillwater, OK, USA, in 1979. He is currently an Associate Professor with the Department of Electrical Engineering, Iran University of Science and Technology, Tehran, Iran. His research interests include reactive power control, power system dynamics, stability and control, and flexible AC transmission systems devices.

MOHAMMAD AMIN GILANI received the B.S. and M.S. degrees in electrical engineering from the Iran University of Science and Technology, in 2014 and 2016, respectively. His research interests include power system optimization, smart grids, demand response, and power system resilience.

MIADREZA SHAFIE-KHAH (Senior Member, IEEE) received the Ph.D. degree in electrical engineering from Tarbiat Modares University, Tehran, Iran, and the Ph.D. degree in electromechanical engineering from the University of Beira Interior (UBI), Covilhã, Portugal. He held his first postdoctoral position at UBI. He also held his second postdoctoral position at the University of Salerno, Fisciano, Italy. He is currently an Associate Professor with the University of Vaasa, Vaasa, Finland. He has coauthored more than 392 articles that received more than 7400 citations with an H-index equal to 48. His research interests include power market simulation, market power monitoring, power system optimization, demand response, electric vehicles, price and renewable forecasting, and smart grids. He is a Top Scientist in the Guide2Research Ranking in computer science and electronics, and he has won five Best Paper Awards at IEEE Conferences. He was considered one of the Best Reviewer of IEEE TRANSACTIONS ON SMART GRID, in 2016 and 2017, and one of the Outstanding Reviewer of IEEE TRANSACTIONS ON SUSTAINABLE ENERGY, in 2014 and 2017, IEEE TRANSACTIONS ON POWER SYSTEMS, in 2017 and 2018, and IEEE OPEN ACCESS JOURNAL OF POWER AND ENERGY (OAJPE), in 2020. He is an Editor of IEEE TRANSACTIONS ON SUSTAINABLE ENERGY and IEEE OPEN ACCESS JOURNAL OF POWER AND ENERGY (OAJPE); an Associate Editor of IEEE SYSTEMS JOURNAL, IEEE ACCESS, and *IET-RPG*; the Guest Editor-in-Chief of IEEE OPEN ACCESS JOURNAL OF POWER AND ENERGY (OAJPE); the Guest Editor of IEEE TRANSACTIONS ON CLOUD COMPUTING and more than 14 Special Issues. He is also the Volume Editor of the book *Blockchain-Based Smart Grids* (Elsevier, 2020).